

Estimating Absolute-Phase Maps Using ESPIRiT and Virtual Conjugate Coils

Martin Uecker¹ and Michael Lustig²

¹Institute for Diagnostic and Interventional Radiology,
University Medical Center Göttingen, Göttingen, Germany.

²German Centre for Cardiovascular Research (DZHK)

³Department of Electrical Engineering and Computer Sciences,
University of California, Berkeley, California.

January 12, 2022

Running head: Estimating Absolute-Phase Maps Using ESPIRiT

Address correspondence to:

Martin Uecker
University Medical Center Göttingen
Institute for Diagnostic and Interventional Radiology
Robert-Koch-Str. 40
37075 Göttingen, Germany
martin.uecker@med.uni-goettingen.de

Supported by: NIH R01EB019241, NIH R01EB009690, NIH P41RR09784, Sloan Research Fellowship, Okawa Research grant, and GE Healthcare.

Approximate word count: 197 (Abstract) 2780 (body)

Submitted to *Magnetic Resonance in Medicine* as a Note.

Part of this work has been presented at the ISMRM Annual Conference 2014.

Abstract

Purpose: To develop an ESPIRiT-based method to estimate coil sensitivities with image phase as a building block for efficient and robust image reconstruction with phase constraints. **Theory and Methods:** ESPIRiT is a new framework for calibration of the coil sensitivities and reconstruction in parallel Magnetic Resonance Imaging (MRI). Applying ESPIRiT to a combined set of physical and virtual conjugate coils (VCC-ESPIRiT) implicitly exploits conjugate symmetry in k-space similar to VCC-GRAPPA. Based on this method, a new post-processing step is proposed for the explicit computation of coil sensitivities that include the absolute phase of the image. The accuracy of the computed maps is directly validated using a test based on projection onto fully sampled coil images and also indirectly in phase-constrained parallel-imaging reconstructions. **Results:** The proposed method can estimate accurate sensitivities which include low-resolution image phase. In case of high-frequency phase variations VCC-ESPIRiT yields an additional set of maps that indicates the existence of a high-frequency phase component. Taking this additional set of maps into account can improve the robustness of phase-constrained parallel imaging. **Conclusion:** The extended VCC-ESPIRiT is a useful tool for phase-constrained imaging.

Key words: parallel imaging, partial Fourier, ESPIRiT, virtual coil

1 Introduction

The primary quantity measured in MRI, the spin density, can be described by a real and positive function. In principle, this prior knowledge can reduce the amount of k-space data necessary to reconstruct an image to one half [8]. In practice, various phase effects from B1, flow, off-resonance, and others cause phase variations in the image. By using a low-resolution phase map, homodyne reconstruction [10] or SENSE-based parallel imaging with a phase constraint can sometimes be applied [11, 22]. Especially in the later case, this causes reconstruction errors if the data is affected by phase variations that are not described by the low-resolution phase map. Recently, ESPIRiT has been described - a new method to obtain highly accurate estimations of the coil sensitivities from a fully-sampled calibration region in the k-space center [17]. The estimates of the maps are defined up to multiplication with an unknown complex-valued function, *i.e.* only relative coil sensitivities are obtained. Here, we demonstrate an extension to ESPIRiT that can be used to estimate coil sensitivities with phase that make the reconstructed image real-valued with high accuracy. This is accomplished by applying ESPIRiT to virtual conjugate coils (VCC-ESPIRiT), which have been introduced previously to improve GRAPPA reconstruction [2, 3]. Instead of doing a reconstruction using virtual conjugate coils which implicitly exploits conjugate symmetry, the new post-processing technique estimates sensitivities with image phase. The reconstruction can then use an explicit real-value constraint as in phase-constrained SENSE which is more flexible and computationally more efficient.

In cases where the image phase is not smooth, phase-constrained SENSE with low-resolution phase maps suffers from reconstruction artifacts. While phase-constrained SENSE has been shown to be equivalent to SENSE with virtual conjugate coils (VCC-SENSE) which suffers from the same problem, methods using calibration in k-space such as ESPIRiT or GRAPPA applied to virtual conjugate coils are more robust [3]. Here, we explain the improved robustness with the appearance of a second eigenvalue in VCC-ESPIRiT, and relate it to the idea of explicitly replacing the hard phase constraint with regularization of the imaginary component [5].

Part of this work has been presented at the 22nd ISMRM Annual Conference [18].

2 Theory

Although the spin density is a positive and real quantity the magnetization image $\rho(\vec{x})$ measured in MRI usually has phase. Formally, the image $\rho(\vec{x})$ can be assumed to be real-valued in the signal equations for parallel imaging if the

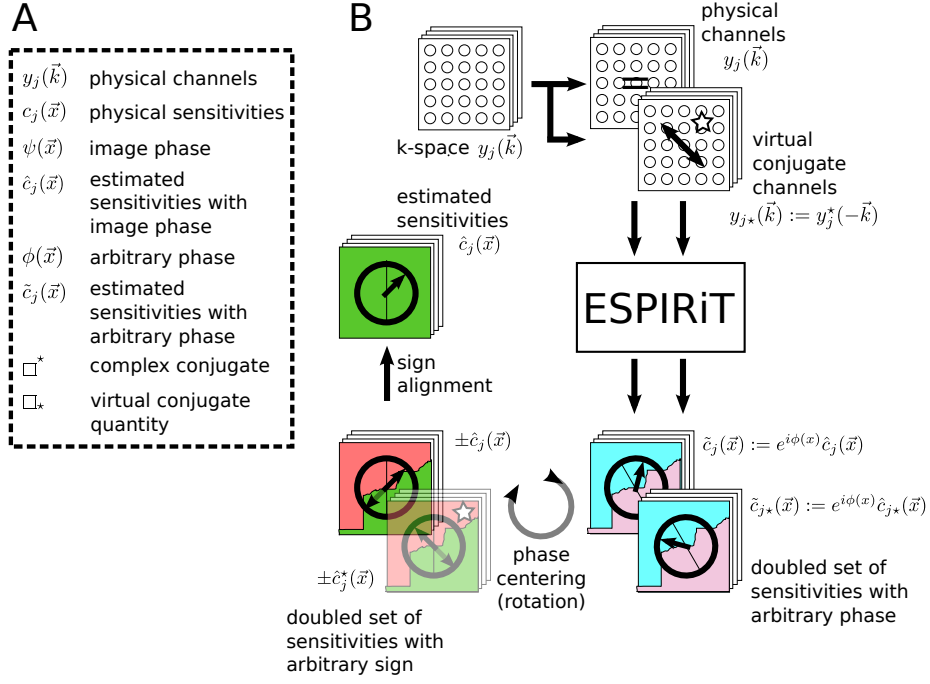


Figure 1: **A:** Important symbols used in the text or in the figure. **B:** Processing steps in the proposed methods (clock-wise): Extension of k-space with additional virtual conjugate coils, ESPIRiT calibration, phase centering, sign unwrapping. After phase centering the virtual channels are redundant and can be discarded.

image phase $\psi(\vec{x})$ is fully absorbed into the coil sensitivities:

$$\begin{aligned}
 y_j(\vec{k}) &= \int d\vec{x} \underbrace{|\rho(\vec{x})| e^{i\psi(\vec{x})}}_{\rho(\vec{x})} c_j(\vec{x}) e^{-i2\pi\vec{k}\cdot\vec{x}} \\
 &= \int d\vec{x} |\rho(\vec{x})| \underbrace{e^{i\psi(\vec{x})} c_j(\vec{x})}_{\hat{c}_j(\vec{x})} e^{-i2\pi\vec{k}\cdot\vec{x}}
 \end{aligned}$$

Here, $y_j(\vec{k})$ represents the k-space sample for the j -th channel at k-space position \vec{k} . $c_j(\vec{x})$ is the physical coil sensitivity map for channel j at image-domain position \vec{x} and \hat{c}_j is the corresponding map with image phase. For example, such maps with image phase can be estimated directly from the k-space center [9], using a recently proposed extension of Walsh’s method [21, 6], or by non-linear inversion with real-value constraint [16]. In this work, we propose an extension to ESPIRiT for the estimation of highly accurate maps with phase. ESPIRiT is a new method for auto-calibrating parallel imaging. It determines the signal space spanned by local patches in k-space using singular value decom-

position of a calibration matrix constructed from auto-calibration data. Because there are local correlations in k-space due to field-of-view (FOV) limitations and correlations induced by the receive coils, this space is a small subspace of the space of all possible patches. ESPIRiT recovers the sensitivity maps of the receive coils as eigenvectors to the eigenvalue one of a single reconstruction operator, which itself is derived from the requirement that all k-space patches lie in the signal subspace. In general, subspace-based methods are highly robust to many types of errors, because the estimated subspace automatically adapts to correlations in the data. In ESPIRiT, multiple sets of sensitivity maps may appear as eigenvectors to the eigenvalue one in case the data does not fit the classical SENSE model. These additional maps can be taken into account in an extended SENSE-like reconstruction which is then as robust as traditional k-space methods. This has been demonstrated for aliasing in the case of a small FOV, motion corruption, and chemical shift [17].

Because the sensitivities are computed as the point-wise eigenvectors of a reconstruction operator, the point-wise joint phase is undefined. Usually, one channel is selected as a reference and for each pixel the phase of all channels is rotated so that the reference has zero phase. With an extension to ESPIRiT, sensitivities with phase \hat{c}_j can be estimated, *i.e.* sensitivities that ideally would result in a real image, as long as noise and other errors are neglected. This is achieved by exploiting the property of ESPIRiT that relative phase between different channels is preserved. The proposed procedure is described in the following and illustrated in Figure 1. By flipping and conjugating k-space virtual conjugate channels

$$y_{j\star}(\vec{k}) := y_j^*(-\vec{k}) = \int d\vec{x} |\rho(\vec{x})| \hat{c}_j^*(\vec{x}) e^{-i2\pi\vec{k}\cdot\vec{x}}$$

are constructed which are then included as additional virtual channels – doubling the total number of channels. ESPIRiT calibration is then applied to the extended data set

$$[y_1(\vec{k}), \dots, y_N(\vec{k}), y_{1\star}(\vec{k}), \dots, y_{N\star}(\vec{k})]$$

to estimate the coil sensitivities for all channels. This yields a vector of sensitivity maps for all physical and virtual sensitivities up to an unknown pixel-wise phase $\phi(\vec{x})$:

$$[\tilde{c}_1(\vec{x}), \dots, \tilde{c}_N(\vec{x}), \tilde{c}_{1\star}(\vec{x}), \dots, \tilde{c}_{N\star}(\vec{x})] = e^{i\phi(\vec{x})} [\hat{c}_1(\vec{x}), \dots, \hat{c}_N(\vec{x}), \hat{c}_{1\star}(\vec{x}), \dots, \hat{c}_{N\star}(\vec{x})]$$

Note that $\phi(\vec{x})$ is an arbitrary phase difference between the estimated sensitivities \tilde{c}_j and the sensitivities with image phase $\hat{c}_j(\vec{x}) = e^{i\psi(\vec{x})} c_j(\vec{x})$, *i.e.* $\tilde{c}_j(\vec{x}) = e^{i(\phi(\vec{x}) + \psi(\vec{x}))} c_j(\vec{x})$. Because conjugate channels $y_{j\star}$ have conjugate sensitivities, *i.e.* $\hat{c}_{j\star}(\vec{x}) = \hat{c}_j^*(\vec{x})$, the unknown phase ϕ can be determined up to π :

$$\frac{1}{2} \text{Im} \log \sum_j \tilde{c}_j(\vec{x}) \tilde{c}_{j\star}(\vec{x}) = \frac{1}{2} \text{Im} \log e^{i2\phi(\vec{x})} \sum_j |c_j(\vec{x})|^2 = \phi(\vec{x}) + l\pi \quad l \in \mathbf{Z}$$

The remaining ambiguity in phase corresponds to unknown sign in the estimated image. When enforcing a real-value constraint in SENSE or in similar reconstructions, the sign ambiguity of the estimated sensitivities can be ignored. In this work, the sign is simply aligned to a low-resolution estimate of the sensitivities. After the estimation of the phase, the virtual conjugate coils are not needed anymore and can be discarded.

A more complicated situation arises if the phase of the image is not smooth, *i.e.* it cannot be represented by a single smooth sensitivity map. In case of such inconsistencies VCC-ESPIRiT automatically produces a second set of sensitivity maps [18, 3]. As shown later, taking this second map into account will essentially relax the phase constraint in affected areas of the image, which can prevent artifacts in phase-constrained reconstructions.

3 Methods

Fully-sampled data from a human brain was acquired with 3D FLASH at 3T (TR/TE = 11/4.9 ms) using a 32-channel head coil and was retrospectively under-sampled with an acceleration factor of $R = 3$ in the first phase-encoding dimension. For some experiments, an additional partial Fourier factor of $PF = 5/8$ was applied in the second phase-encoding direction. Except where stated differently, experiments used a calibration region consisting of 24x24 auto-calibration signal (ACS) lines.

The Berkeley Advanced Reconstruction Toolbox (BART) was used for calibration and image reconstruction [19].¹ In the interest of reproducible research, code and data to reproduce the experiments are made available on Github.² Sensitivity maps were computed using direct estimation from the k-space center [9], ESPIRiT, and the proposed VCC-ESPIRiT method. For both ESPIRiT-based methods the following default parameters were used: The kernel size was six and the null-space threshold in the first step of the ESPIRiT calibration was 0.001 of the maximum singular-value [17]. For image reconstruction, maps were weighted with a smooth S-curve transition between one and 0.85 of the local eigenvalue [20]. In this work, the unknown sign is irrelevant and has simply been aligned to a low-resolution reference to avoid visually distracting sign jumps. The quality of the estimated maps was directly evaluated in dependence of the kernel size and the size of the calibration region. For the evaluation, extended versions of a previously described projection test can be used [17]: Coil images m_j obtained with discrete Fourier transform from fully sampled data were projected onto the span of normalized sensitivity maps by summing the images after multiplication with conjugate sensitivities and then multiplying with the sensitivities again.

$$(Pm)_j(\vec{x}) = \frac{\hat{c}_j(\vec{x}) \sum_{t=1}^N \hat{c}_t^*(\vec{x}) m_t(\vec{x})}{\sum_{s=1}^N |\hat{c}_s(\vec{x})|^2}$$

¹<https://mrirecon.github.io/bart/>

²<https://github.com/uecker/vcc-espirit/>

This operation is also one of the projections repeatedly applied in POCSense [13]. The result of the projection $(Pm)_j$ is then subtracted from the original coil images to obtain error maps $E_j(\vec{x}) = m_j(\vec{x}) - (Pm)_j(\vec{x})$ where any remaining signal different from noise indicates that the maps do not span the data space correctly. The error maps for all channels can be combined into a single error map according to the root-sum-of-squares formula $\sqrt{\sum_j |E_j|^2}$. This procedure can be extended to test how well the maps describe the image phase by including a projection onto the real part of the image:

$$(P_R m)_j(\vec{x}) = \frac{\hat{c}_j(\vec{x}) \operatorname{Re} \sum_{t=1}^N \hat{c}_t^*(\vec{x}) m_t(\vec{x})}{\sum_{s=1}^N |\hat{c}_s(\vec{x})|^2}$$

As another extension, projecting onto the span of multiple sets can simply be achieved by summing all individual projections.

Iterative reconstruction with a phase constraint was performed for different sampling schemes and slices. Reconstructions using one set of VCC-ESPIRiT maps or two sets of VCC-ESPIRiT maps were compared with directly estimated maps [9]. In addition, regularization of the imaginary component instead of a hard phase constraint was used [5]. To evaluate the reconstruction error including phase errors difference images were computed in the following way: Individual coil images were computed by multiplying the reconstructed images with the sensitivities. Then, for each channel the difference to the corresponding coil image from fully-sampled k-space data was computed. Finally, the difference images for all channels were combined using root-sum-of-squares formula.

4 Results

Figure 2 shows individual coil images and the first two sets of maps computed with VCC-ESPIRiT for the first eight channels of the brain data set. The primary set of maps represents the coil sensitivities with image phase which matches the phase of the coil images except for high-frequency phase components. A second set of maps appears in image regions affected by this high-frequency phase, which - in this example - is caused by off-resonance from fat. Figure 3 shows the results of the projection test for the VCC-ESPIRiT maps. The real projection P_R of the coil images onto the space spanned by the coil sensitivities shows that the image and coil phase are accurately captured in most parts of the image, but that residual signal occurs in areas with high-frequency phase from fat and blood vessels which cannot be modelled with a single set of smooth maps even with a larger calibration region. With a second set of maps a larger space is spanned and the residual signal can be modelled. Although the quality of the maps degrades if the calibration region is smaller than 24×24 and especially when a large kernel size is used together with a small calibration region, the quality of the single set of VCC-ESPIRiT maps is otherwise relatively robust to the choice of parameters. When using just a single set of maps, increasing the calibration region and the kernel size does

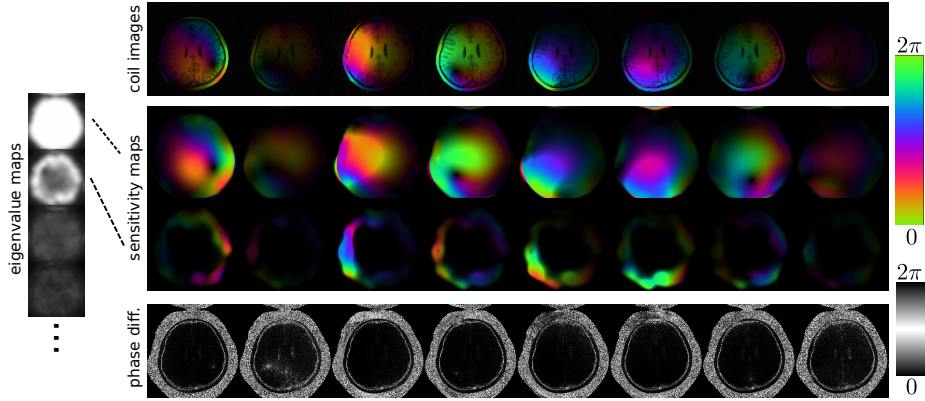


Figure 2: VCC-ESPIRiT was applied to a calibration region of size 24×24 of a human brain data set. **Left:** The first four from 64 eigenvalue maps from VCC-ESPIRiT calibration. In some regions a second eigenvalue close to one indicates the existence of a second set of maps. **Right:** Coil images, the first and second set of sensitivity (eigenvector) maps, and a phase-difference map between the coil images and the first set of maps are shown (only the first eight out of 32 physical channels are shown). Except for the phase-difference map the phase is encoded using color.

not improve the error much. This is because high frequency phase can not be represented well without going to extreme sizes. In contrast, increasing the calibration region and kernel sizes does reduce the error when two sets of maps are used. In our example, for 40×40 calibration region using two sets of maps, while enforcing real-valued result, has comparable error to the case where phase is not constrained. This means that for this case, VCC-ESPIRiT captures well the signal subspace with all its phase variations.

Figure 4 demonstrates reconstruction of data from an accelerated parallel-imaging and a parallel-imaging partial-Fourier acquisition using differently estimated maps and various constraints. When using a single set of maps together with a real-value constraint, aliasing artifacts are not completely resolved in the reconstruction (B,E,F,H,K,L). By using a second set of VCC-ESPIRiT maps the real-value constraint is relaxed in image regions affected by high-frequency phase. In this example, this yields reconstructions almost without visible artifacts (C,I). Good reconstructions can also be obtained when the real-value constraint is generally replaced by regularization of the imaginary component (D,J). Comparing the results using VCC-ESPIRiT maps with results using directly estimated maps (EF,KL) confirms the better accuracy of ESPIRiT maps. Even when using regularization of the imaginary part minor artifacts remain in the case of directly estimated maps. For the partial Fourier case, the iterative reconstruction without real-value constraint shows pronounced blurring due to the missing information in one half of k-space (G). Using a real-value constraint

or regularization of the imaginary part yields sharp images (H-L).

In Figure 5 reconstructed images for a slice with more phase variations are shown. Although the reconstruction using two sets of VCC-ESPIRiT maps has significantly reduced errors compared to the reconstruction using only one set of maps, it still fails to recover a good image due to unaccounted phase. The combination of a single set of VCC-ESPIRiT maps with regularization of the imaginary component yields a good reconstruction.

5 Discussion

This work describes VCC-ESPIRiT, an extension to ESPIRiT for the computation of sensitivity maps which include image phase. It combines ESPIRiT applied to virtual conjugate channels with a post-processing step to determine the phase of the maps. Having explicit sensitivities with image phase is useful in a wide variety of image reconstruction tasks. In phase-constrained reconstruction it can be used to exploit conjugate symmetry to increase SNR or recover information from partial-Fourier acquisitions. In model-based image reconstruction the phase of the image must often be taken into account in the forward model.

Especially when only a limited amount of calibration data is available, ESPIRiT maps are often more accurate than maps directly estimated from the k-space center [17]. Still, even with ESPIRiT maps phase-constrained parallel imaging with a single set of maps is not robust to errors from high-frequency phase variations which cannot be described by a smooth map. It has been shown previously that k-space methods based on virtual conjugate coils are more robust [3]. Using the ESPIRiT formalism this observation can be explained: In regions of the image with high-frequency phase variations the reconstruction operator has a second eigenvalue close to the value one. The corresponding eigenvector map corresponds to a second set of maps that is needed to span the data - indicating the location where the imaginary component of the signal cannot be neglected. As shown, using the second set of maps in a real-value constrained reconstruction is more robust, because it relaxes the constraint at the corresponding locations to allow arbitrary complex values. Interestingly, this works because the approximate location of small objects with high-frequency phase such as blood vessels can be recovered from a relatively small amount of data from the k-space center. This property can be explained by the relationship of ESPIRiT to classical subspace-based frequency-estimation methods [14, 12].

As long as only high-frequency phase variations but no other kinds of corruption occur, the essential information are the locations where the real-value constraint has to be relaxed. Although the real-value constraint could be modified directly, using multiple sensitivity maps has the advantage of being robust also against other types of errors. It should be noted that with other types of errors the multiple sets of maps might appear as an arbitrary linear mixture of eigenvectors to eigenvalue one [17, 1]. If this is the case, the maps are usually not smooth due to mixing of different components. If smooth maps are desired, *e.g.* when sparsity

constraints are applied to the coil-combined image, additional alignment steps similar to the ones proposed for ESPIRiT-based coil compression are needed [1]. For images with a large amount of phase variations using two ESPIRiT maps estimated from low-resolution calibration data still does not sufficiently relax the constraints for an artifact-free reconstruction. In this case, it is necessary to replace the hard phase constraint with an increased regularization of the imaginary component, *i.e.* softening the constraint everywhere [5]. Although the information from the second map is then not required, this method still critically depends on accurate phase information and benefits from the higher accuracy of the sensitivities estimated with ESPIRiT. As another enhancement, a sparsity penalty applied directly to the imaginary component may allow further improvements [7].

If not enough calibration information is available, another reconstruction method can be used to first recover a larger calibration area from partially under-sampled k-space center, for example using iterative GRAPPA [3] or (robust) SAKE [15, 23]. To exploit correlations between conjugate-symmetric parts of k-space at this stage, this could be applied to a k-space already extended with virtual conjugate coils, *i.e.* using VCC-SAKE. In fact, a very similar method called LORAKS has recently been proposed [4].

Finally, if the phase is of interest in itself, *i.e.* in phase-contrast imaging, a possible approach is to synthesize regular coil images from the reconstructed image by multiplying with the sensitivities. The synthetic coil images then include all phase information and can be further processed as with other methods. Of course, the use of any type of phase constraint must be considered very carefully in these applications.

6 Conclusion

An extension to ESPIRiT has been presented, which can be used to estimate coil sensitivities which include slowly-varying image phase. The sensitivities with phase can be directly used in a reconstruction with real-value constraint to improve SNR or to exploit conjugate-symmetry in k-space for partial Fourier acquisitions. In case of high-frequency phase variations, VCC-ESPIRiT yields a second set of maps in affected regions, which can then be taken into account to make phase-constrained reconstructions more robust. If the image has a large amount of high-frequency phase, robust reconstruction requires the phase constraint to be relaxed.

Acknowledgements

The authors thank Mariya Doneva for valuable comments.

References

- [1] D. Bahri, M. Uecker, and M. Lustig. Three-nearest-neighbor alignment for smooth ESPIRiT maps. In *Proceedings of the 22nd Annual Meeting ISMRM*, page 4394, Milano, 2014.
- [2] M. Blaimer, M. Gutberlet, P. Kellman, F. A. Breuer, H. Köstler, and M. A. Griswold. Virtual coil concept for improved parallel MRI employing conjugate symmetric signals. *Magn Reson Med*, 61:93–102, 2009.
- [3] M. Blaimer, M. Heim, D. Neumann, P. M. Jakob, S. Kannengiesser, and F. A. Breuer. Comparison of phase-constrained parallel MRI approaches: Analogies and differences. *Magn Reson Med*, 2015. Epub, doi: 10.1002/mrm.25685.
- [4] J. P. Haldar. Low-rank modeling of local k -space neighborhoods (LO-RAKS) for constrained MRI. *IEEE Trans Med Imaging*, 33:668–681, 2014.
- [5] W. S. Hoge, M. E. Kilmer, C. Zacarias-Almarcha, and D. H. Brooks. Fast regularized reconstruction of non-uniformly subsampled partial-fourier parallel mri data. In *Biomedical Imaging: From Nano to Macro (ISBI). 4th IEEE International Symposium on*, pages 1012–1015, Washington, 2007.
- [6] S. J. Inati, M. S. Hansen, and P. Kellman. A solution to the phase problem in adaptive coil combination. In *Proceedings of the ISMRM 21th Annual Meeting*, page 2672, Salt Lake City, 2013.
- [7] G. Li, J. Hennig, E. Raithel, M. Büchert, D. Paul, J. G. Korvink, and M. Zaitsev. An L1-norm phase constraint for half-Fourier compressed sensing in 3D MR imaging. *Magnetic Resonance Materials in Physics, Biology and Medicine*, 28:459–472, 2015.
- [8] P. Margosian, F. Schmitt, and D. Purdy. Faster MR imaging: imaging with half the data. *Health Care Instrum*, 1:195, 1986.
- [9] C.A. McKenzie, E.N. Yeh, M.A. Ohliger, M.D. Price, and D.K. Sodickson. Self-calibrating parallel imaging with automatic coil sensitivity extraction. *Magn Reson Med*, 47:529–538, 2002.
- [10] D. C. Noll, D. G. Nishimura, and A. Macovski. Homodyne detection in magnetic resonance imaging. *IEEE Trans Med Imaging*, 10:154–163, 1991.
- [11] K. P. Pruessmann, M. Weiger, M. B. Scheidegger, and P. Boesiger. SENSE: Sensitivity encoding for fast MRI. *Magn Reson Med*, 42:952–962, 1999.
- [12] R. Roy and T. Kailath. ESPRIT - Estimation of signal parameters via rotational invariance techniques. *IEEE Trans Acoust Speech Signal Process*, 37:984–995, 1989.

- [13] A. A. Samsonov, E. G. Kholmovski, D. L. Parker, and C. R. Johnson. POCSENSE: POCS-based reconstruction for sensitivity encoded magnetic resonance imaging. *Magn Reson Med*, 52:1397–1406, 2004.
- [14] R. O. Schmidt. Multiple emitter location and signal parameter estimation. *IEEE Trans Antennas Propag*, 34:276–280, 1986.
- [15] P. J. Shin, P. E. Z. Larson, M. A. Ohliger, M. Elad, J. M. Pauly, D. B. Vigneron, and M. Lustig. Calibrationless parallel imaging reconstruction based on structured low-rank matrix completion. *Magn Reson Med*, 72:959–970, 2014.
- [16] M. Uecker, A. Karaus, and J. Frahm. Inverse reconstruction method for segmented multishot diffusion-weighted MRI with multiple coils. *Magn Reson Med*, 62:1342–1348, 2009.
- [17] M. Uecker, P. Lai, M. J. Murphy, P. Virtue, M. Elad, J. M. Pauly, S. S. Vasanawala, and M. Lustig. ESPIRiT – an eigenvalue approach to auto-calibrating parallel MRI: Where SENSE meets GRAPPA. *Magn Reson Med*, 71:990–1001, 2014.
- [18] M. Uecker and M. Lustig. Robust partial Fourier parallel imaging using ESPIRiT and virtual conjugate coils. In *Proceedings of the 22nd Annual Meeting ISMRM*, volume 22, page 1629, Milano, 2014.
- [19] M. Uecker, F. Ong, J. I. Tamir, D. Bahri, P. Virtue, J. Y. Cheng, T. Zhang, and M. Lustig. Berkeley advanced reconstruction toolbox. In *Proceedings of the 23rd Annual Meeting ISMRM*, volume 23, page 2486, Toronto, 2015.
- [20] M. Uecker, P. Virtue, S. S. Vasanawala, and M. Lustig. ESPIRiT reconstruction using soft SENSE. In *Proceedings of the 21st Annual Meeting ISMRM*, volume 21, page 127, Salt Lake City, 2013.
- [21] D. O. Walsh, A. F. Gmitro, and M. W. Marcellin. Adaptive reconstruction of phased array MR imagery. *Magn Reson Med*, 43:682–690, 2000.
- [22] J. D. Willig-Onwuachi, E. N. Yeh, A. K. Grant, M. A. Ohliger, C. A. McKenzie, and D. K. Sodickson. Phase-constrained parallel MR image reconstruction. *J Magn Reson*, 176:187–198, 2005.
- [23] D. Zhu, M. Uecker, J. Y. Cheng, Z. Bi, K. Ying, and M. Lustig. Calibration for parallel MRI using robust low-rank matrix completion. In *Proceedings of the 22nd Annual Meeting ISMRM*, volume 22, page 741, Milano, 2014.

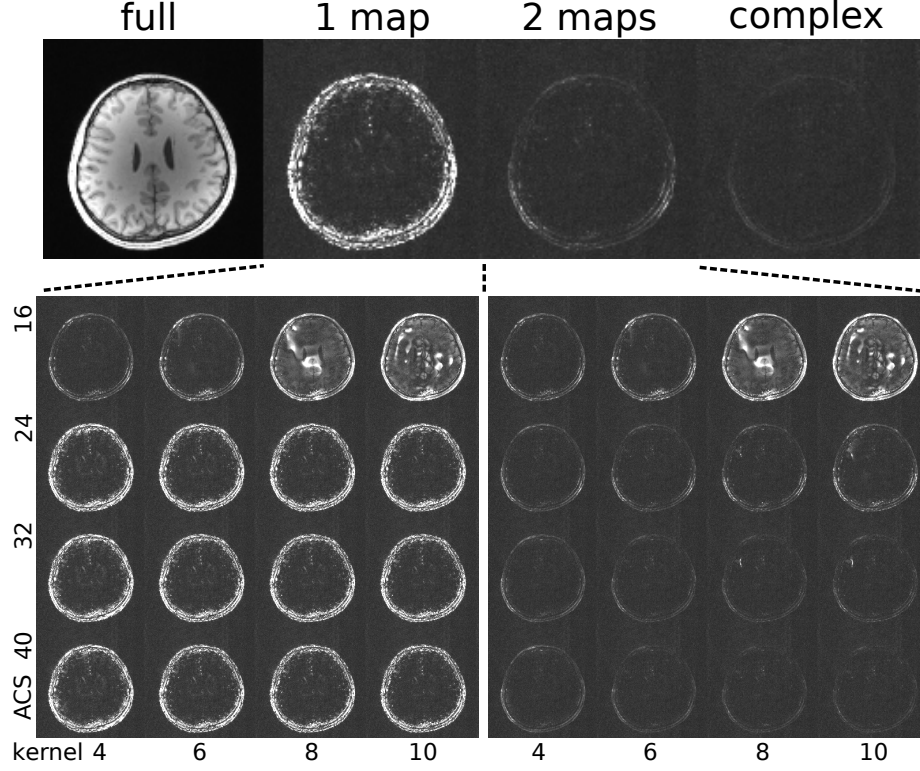


Figure 3: This figure shows the combined residual (unexplained) signal from all channels after projection of the coil images onto different spaces. **Top:** full signal for comparison (full), real-projection onto the first set of VCC-ESPIRiT maps (1 map), real-projection onto both sets of VCC-ESPIRiT maps (2 maps), complex-projection onto a single set of conventional ESPIRiT maps (complex). **Bottom:** The impact of the size of the calibration region and the size of the kernel on the quality of the maps is evaluated using a real-projection onto one (left) or both (right) sets using a calibration region (ACS) of size 16x16, 24x24, 32x32, and 40x40 and kernel size of 4x4, 6x6, 8x8, and 10x10. For each case, the residual signals for all channels have been combined into a single image using the root-sum-of-squares method. Relative to the full signal all other images have been scaled up by a factor of five to aid visualization.

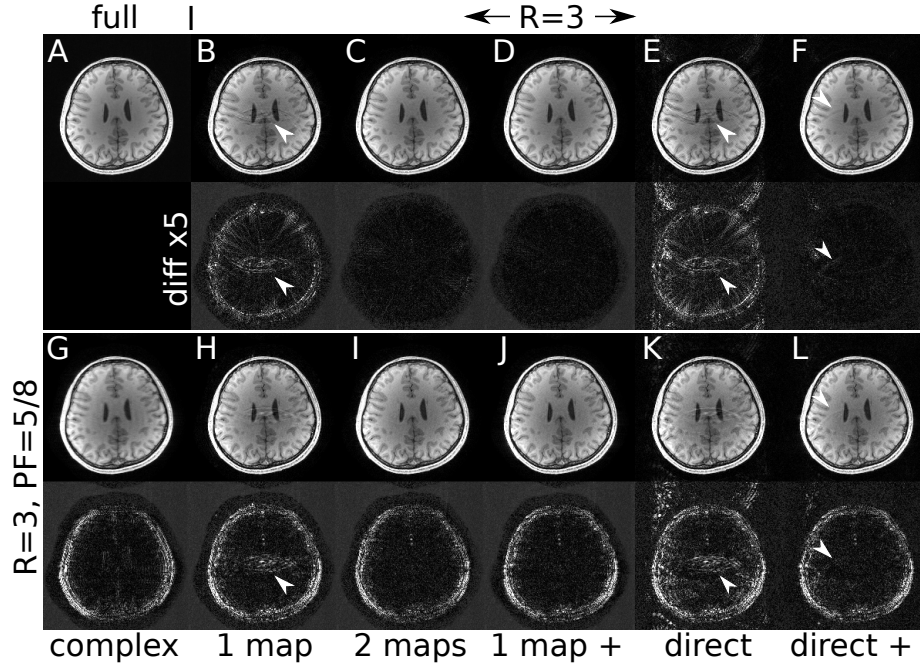


Figure 4: Reconstruction from fully-sampled data (A) and iterative parallel imaging reconstruction ($R = 3$, 24×24 ACS lines) with (top, B-F) and without (bottom, G-L) additional partial-Fourier sampling ($PF=5/8$). Sensitivities were estimated with VCC-ESPIRiT using one set of maps (1 map, B,H,D,J) or two set of maps (2 maps, C,I) or directly from the k-space center (direct, E,F,K,L). Some variants use regularization of the imaginary component (indicated by +, D,J,F,L) or no phase constraint (complex, G). If the high-frequency phase of the image is not correctly modelled, a real-value constraint causes artifacts (arrows). Difference images to the fully-sampled reference are scaled up by a factor of five.

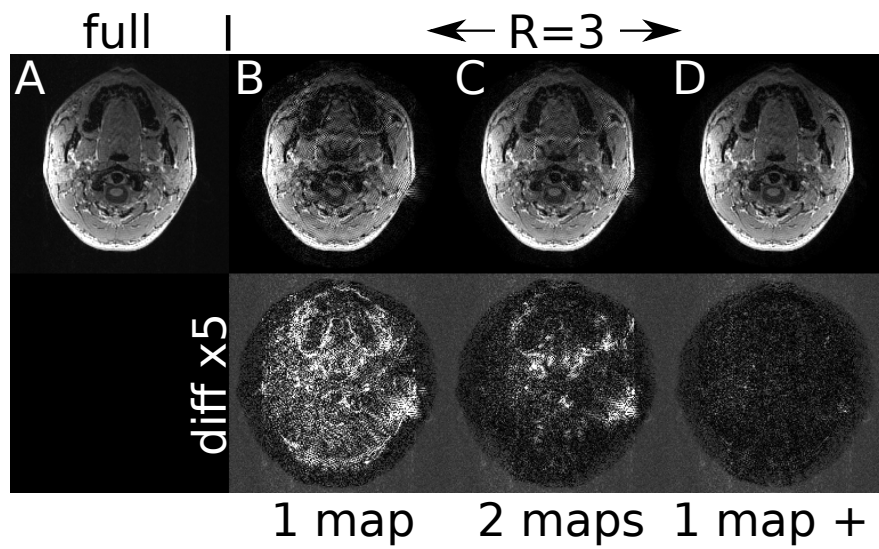


Figure 5: Reconstruction from fully-sampled data (full, A), VCC-ESPIRiT using one set of maps (1 map, B), VCC-ESPIRiT using two set of maps (2 maps, C), and VCC-ESPIRiT using one set of maps with regularization of the imaginary component (1 map +, D). Difference images to the fully-sampled reference are scaled up by a factor of five.